Nondisruptive decentralized control of thermal loads with second order thermal models

Simon H. Tindemans and Goran Strbac
Department of Electrical and Electronic Engineering
Imperial College London
London, United Kingdom
s.tindemans@imperial.ac.uk

***Abstract*—Dynamic load controllers for thermostatically controlled loads should allow for accurate control of power consumption and should not disrupt the quality of service. This paper proposes an intuitive definition of nondisruptiveness for systems with second-order thermal models, based on a decomposition into fast and slow temperature modes. It enables the explicit control of the slow mode temperature using an embedded first order model; control of the fast mode is implicit. Temperature bounds are derived, and the slow mode controller is implemented using an accurate decentralised stochastic control strategy. Simulation results confirm its accuracy and nondisruptiveness.**

***Index Terms*—aggregate load control, demand-side management, nondisruptive control, thermal models, thermostatically controlled loads**

I. Introduction

Collectively, thermostatically controlled loads (TCLs) such as refrigerators, freezers, space heaters and air conditioners present a significant source of load flexibility. This flexibility can assist in system balancing, or to locally provide voltage support or relax thermal constraints. However, it remains an open question how this flexibility should be made available to the system. A good control scheme should provide accurate control of the TCLs' aggregate power consumption without onerous communication requirements, and – most importantly – it should be *nondisruptive*, i.e. it must not interfere with the primary function of the appliances [1].

In order to optimally balance system level objectives with device level constraints, it is essential to correctly model these quality of service constraints. In recent work on advanced control strategies, TCLs have often been represented by first order thermal models consisting of a temperature-controlled compartment and an ambient temperature [2], [3], where the compartment should stay within strict temperature bounds. Zhang *et al.* did explicitly consider constraints in two-dimensional thermal models, but their control approach relied on centralised state estimation and real-time communication [4], which may impede practical implementation.

In this paper we adapt the nondisruptive decentralised TCL controller developed in [3] to control devices with second order thermal models. We demonstrate that an appropriate linear transformation can separate the second order dynamics into fast and slow temperature modes that are mutually independent except for their dependence on the common on/off signal. The device can be controlled using a first order control model for the slow mode only, making use of appropriate effective temperature constraints. The fast mode decays more rapidly and is naturally bounded by the limits on the slow mode. The notion of nondisruptiveness is adapted to this decomposition: we derive slow mode constraints from steady state operations, and further derive a two-dimensional temperature envelope that is respected under all conditions by this control strategy. Simulation results demonstrate the ability to track desired power profiles, while respecting the computed temperature envelope at all times.

II. Second order thermal models

In this paper we consider second order thermal models with two temperature variables (T_1 and T_2) and a single control signal $s(t)$. For a non-varying model, the temperature evolution takes the form of an inhomogeneous coupled system of linear differential equations:

$$\frac{\mathrm{d}}{\mathrm{d}t}\begin{pmatrix}T_1\\T_2\end{pmatrix} = M\cdot\begin{pmatrix}T_1\\T_2\end{pmatrix} + s(t)\vec{b}_{\mathrm{on}} + (1-s(t))\vec{b}_{\mathrm{off}}. \qquad (1)$$

For the purpose of this paper we will assume that individual appliances have an on/off controller, so that the control signal is binary: $s(t)$ is either 0 (off) or 1 (on). This restriction reflects the behaviour of common refrigerators and air conditioners.

A. A refrigeration example

Second order thermal models naturally arise from bottom-up modelling of systems with two thermal zones that interact with each other – and usually with an external reservoir (e.g. the ambient). Two examples of such systems are shown in Figure 1. In addition, second order models are also a natural choice for phenomenological model matching in cases where first order models are not sufficient to capture the relevant dynamics of a system. Zhang *et al.* [4] convincingly argued for the importance of considering second order thermal models for flexible air conditioning loads.

Using a common linear approximation, the passive heat flow $\dot{Q}_{ab}$ [J/s] between zones a and b is proportional to the temperature difference $T_a - T_b$ divided by the thermal resistance R_{ab} [Ks/J]. The impact of this heat flow on temperatures T_a

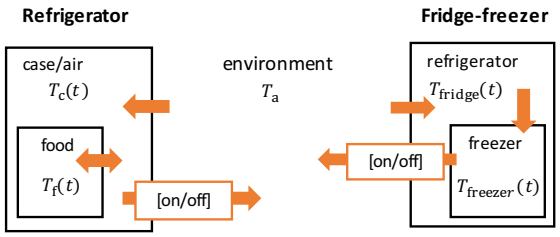

Fig. 1. Depictions of two heat exchange models that correspond to a second order representation: refrigerator with case/food distinction (left) and fridge/freezer (right). The flow of heat is indicated by orange arrows.

and T_b is determined by the thermal capacities C_a and C_b [J/K], respectively. To illustrate this generic approach to model construction (also known as Equivalent Thermal Parameter (ETP) modelling [4]), we consider a second order model for a refrigerator with stored food (see Fig. 1). The three zones have temperatures T_a (ambient; assumed constant), $T_c(t)$ (case) and $T_f(t)$ (food), with associated thermal capacities C_c and C_f. Passive heat flows exist between the case and exterior (resistance R_{ac}), and between the case and food (resistance R_{cf}). The heat extraction by the refrigeration cycle gives rise to an additional heat flow F_{on} [J/s] from the case to the environment. The resulting thermal model is

$$\frac{\mathrm{d}}{\mathrm{d}t}\begin{pmatrix}T_c(t)\\T_f(t)\end{pmatrix} = \begin{pmatrix}-\frac{1}{C_c}\left[\frac{1}{R_{ac}}+\frac{1}{R_{cf}}\right] & \frac{1}{C_c R_{cf}}\\ \frac{1}{C_f R_{cf}} & -\frac{1}{C_f R_{cf}}\end{pmatrix}\cdot\begin{pmatrix}T_c(t)\\T_f(t)\end{pmatrix} + s(t)\begin{pmatrix}\frac{1}{C_c}\left[\frac{T_a}{R_{ac}}-F_{\text{on}}\right]\\0\end{pmatrix} + (1-s(t))\begin{pmatrix}\frac{T_a}{C_c R_{ac}}\\0\end{pmatrix} \quad (2)$$

In the remainder of this paper, results will be illustrated with the above model, using parameter values from [5]. In the notation of (1), these values result in the system parameters

$$M = \begin{pmatrix}-0.000705 & 0.000556\\ 0.000104 & -0.000104\end{pmatrix} \quad [1/\text{s}] \quad (3a)$$

$$\vec{b}_{\text{on}} = \begin{pmatrix}-0.00643\\0\end{pmatrix}, \qquad \vec{b}_{\text{off}} = \begin{pmatrix}0.00297\\0\end{pmatrix} \quad [\text{K/s}] \quad (3b)$$

B. Spectral decomposition

The analysis and subsequent control of the second order model (1) is greatly simplified by a spectral decomposition of the equations. For a non-trivial system that interacts with an external reservoir, the matrix M has two distinct eigenvalues λ_1 and λ_2 and may be diagonalised as $M = Q\cdot\Lambda\cdot Q^{-1}$, where Λ is the diagonal matrix of eigenvalues and the columns of Q are the corresponding eigenvectors. This suggests the natural coordinate transformation $\vec{u} \equiv Q^{-1}\cdot\vec{T}$, allowing (1) to be written as

$$\frac{\mathrm{d}}{\mathrm{d}t}\vec{u}(t) = \Lambda\cdot\vec{u}(t) + s(t)\vec{c}_{\text{on}} + (1-s(t))\vec{c}_{\text{off}}, \quad (4)$$

where $\vec{c}_{[\text{on/off}]} = Q^{-1}\cdot\vec{b}_{[\text{on/off}]}$. Because Λ is diagonal, the dynamics of temperature components u_1 and u_2 is uncoupled, except for their common dependence on $s(t)$.

1) Slow and fast modes: Physical systems that are connected to an external reservoir are inherently stable, which means both eigenvalues are negative and may be interpreted as (inverse) thermal relaxation time constants. Thus we define the slow and fast time constants

$$\tau^{\text{slow}} = 1/\min_i(-\lambda_i), \qquad \tau^{\text{fast}} = 1/\max_i(-\lambda_i) \quad (5)$$

For the parameters in (3), the thermal relaxation times are $\tau^{\text{slow}} = 14.15$ hours and $\tau^{\text{fast}} = 21.1$ minutes. This illustrates the extent to which the slow and fast dynamics differ - a property that will be used in subsequent sections to simplify the control formulation.

2) Numerical considerations: There are two degrees of freedom in choosing the normalisation of both eigenvectors in Q. We propose a normalisation that results in a natural correspondence in scale between $\vec{u}$ and $\vec{T}$. This is achieved by enforcing that the 1-norm of *each row* of Q^{-1} equals one. For the parameters (3) this choice results in the transformation

$$u^{\text{slow}}(t) = 0.13\ T_c(t) + 0.87\ T_f(t) \quad (6a)$$

$$u^{\text{fast}}(t) = 0.55\ T_c(t) - 0.45\ T_f(t) \quad (6b)$$

It is clear that the slow mode temperature u^{slow} may be interpreted as a weighted average temperature of the system as whole. The temperature u^{fast}, on the other hand, represents the temperature difference between the case and the food. It is intuitive that the internal equilibration of the temperature (the fast mode) is much more rapid than the heating or cooling of the system as a whole (the slow mode).

III. Nondisruptive control for 2nd order systems

Having analysed the system's thermal response, we now consider which limitations must be imposed on the control signal $s(t)$ in order to guarantee the provision of adequate cooling. Domestic refrigerators typically feature a temperature deadband controller (hysteresis controller) that approximately maintains a monitored temperature $T(t)$ (e.g. a single thermal zone) at a setpoint temperature T_{set}. It does so by switching the compressor *on* when a maximum temperature $T_{\max} > T_{\text{set}}$ is exceeded and *off* when the temperature drops below $T_{\min} < T_{\text{set}}$. This results in the quality of service constraint

$$T_{\min} \le T(t) \le T_{\max}. \quad (7)$$

For our illustrative refrigerator, the temperature being monitored is the case temperature $T_c(t)$, and the associated temperature deadband is

$$[T_{\min}, T_{\max}] = [2°C, 7°C]. \quad (8)$$

The resulting steady state temperature traces for both the case and food are shown in Figure 2 (top). Clearly, fluctuations of the case temperature far exceed those of the food temperature. An approximate first order model is shown alongside it for comparison.

Load control using thermostatic loads is a secondary benefit of the primary service of heating/cooling. Ideally, the provision

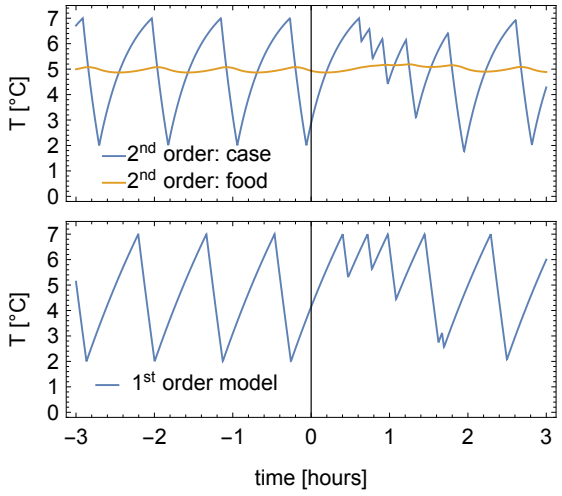

Fig. 2. Temperature dynamics of a second order refrigerator model specified by (3) and (8) (top) and its approximate first order model (bottom) [8, domestic refrigerator]. Both models initially operate in a regular hysteresis loop ($t < 0$) and begin modulating their load following a load management event at $t = 0$.

of energy services should be *nondisruptive*, which means it has "an imperceptible effect on end-use performance" [1]. The qualitative goal of a nondisruptive controller has been implemented in different ways. For example, Ramanathan and Vittal [6] aim to fairly distribute discomfort. Mathieu *et al.* [7], Zhang *et al.* [4] and Tindemans *et al.* [3] enforce appliance temperatures to remain within the regular deadband (7) at all times. Trovato *et al.* [8] impose an additional constraint on the long-term average temperature of appliances.

In this paper, we propose an alternative definition of nondisruptiveness for second order systems. Instead of constraining one of the zonal temperatures using (7) we define nondisruptiveness in terms of the slow temperature mode of the system:

$$u^{\text{slow}}_{\min} \leq u^{\text{slow}}(t) \leq u^{\text{slow}}_{\max} \tag{9}$$

Clearly, this is not an identical replacement of (7), but we will show that $u^{\text{slow}}_{\min}$ and $u^{\text{slow}}_{\max}$ can be chosen such that case/food temperature excursions are strictly bounded and the *steady state* hysteresis loop is identical to the regular controller.

Because the fast and slow modes are decoupled and (9) affects only a single mode, the system may be controlled *as if it were* a first order system. It follows from (4) that the first order system is defined by the differential equation

$$\frac{\mathrm{d}u^{\text{slow}}(t)}{\mathrm{d}t} = -\frac{1}{\tau^{\text{slow}}}u^{\text{slow}}(t) + s(t)c^{\text{slow}}_{\text{on}} + (1-s(t))c^{\text{slow}}_{\text{off}} \tag{10}$$

and the constraint (9). We note that there are no explicit constraints on the fast mode; instead, the value of $u_{\text{fast}}(t)$ is slaved to the control of the slow mode through the on/off signal $s(t)$ and the differential equation

$$\frac{\mathrm{d}u^{\text{fast}}(t)}{\mathrm{d}t} = -\frac{1}{\tau^{\text{fast}}}u^{\text{fast}}(t) + s(t)c^{\text{fast}}_{\text{on}} + (1-s(t))c^{\text{fast}}_{\text{off}} \tag{11}$$

The rapid relaxation of the fast mode ($\tau^{\text{fast}} \ll \tau^{\text{slow}}$) ensures that its excursions are bounded (Section III-B).

Associating the quality of service constraint with the slow mode has two distinct advantages. The first is that the embedded first order thermal model results in a considerable simplification of the control problem. The second advantage is that a constraint of the form (9) may in fact be a more accurate description of the temperature *control intent*. Whereas a temperature constraint of the form (7) affects only a single temperature zone, the slow mode $u^{\text{slow}}(t)$ represents a weighted average of temperatures, including, in our example, the actual temperature of the food.

Naturally, implementing a controller along the u^{slow}-coordinate requires appliances to act on the current value of $u^{\text{slow}}(t)$. In general, this value cannot be determined on the basis of a single temperature measurement (e.g. the case temperature), so it must be estimated using historical measurements and an internal model representation. Alternatively, smart TCLs could be fitted with additional temperature sensors to make this task easier. For the purpose of this paper, we will assume that the thermal model is constant and that the value of $u^{\text{slow}}(t)$ can be inferred with sufficient accuracy.

The remainder of this section is concerned with analysing the temperature excursions that may be observed when the system (10)-(11) is operated with the constraint (9). We derive a two-dimensional temperature envelope Ω_T that bounds the realised temperatures (T_c, T_f) for *any* permitted control strategy. Its construction is visualised in Figure 3.

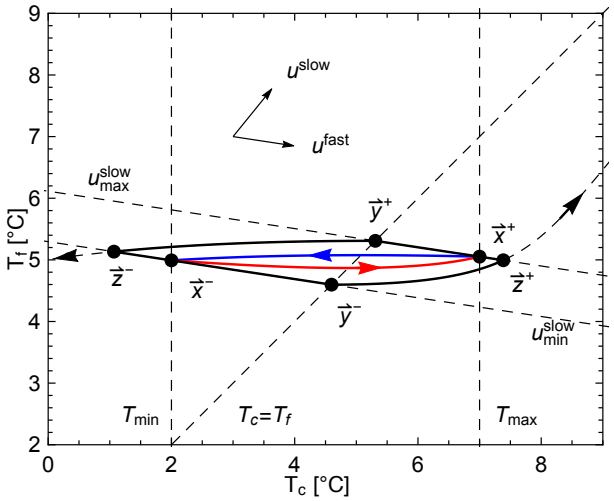

Fig. 3. Temperature dynamics of a second order refrigerator model subjected to a power modulation control signal. The solid black line delineates the permissible temperature envelope Ω_T, and the red and blue arrows depict the steady state off and on cycles, respectively.

A. Limits on the slow mode

Appropriate limit values $u^{\text{slow}}_{\min}$ and $u^{\text{slow}}_{\max}$ for the slow mode will be computed from the steady state operation of the regular hysteresis controller. The steady state switching points $\vec{x}^+ = (T_{\max}, T_f^{ss+})^T$ and $\vec{x}^- = (T_{\min}, T_f^{ss-})^T$ are the temperature-pairs (e.g. case and food) where the refrigerators switch on

and off, respectively. Define $\phi(t;\vec{T}_0,s)$ as the solution of (1) from an initial temperature $\vec{T}(0)=\vec{T}_0$ and a constant control state s. Then, T_f^{ss+} and T_f^{ss-} are implicitly defined by

$$\vec{x}^{+} = \phi(t_1;\vec{x}^{-},0) \tag{12}$$

$$\vec{x}^{-} = \phi(t_2;\vec{x}^{+},1) \tag{13}$$

for some value of t_1, t_2. The switching points and their connecting trajectories (red for heating/off, blue for cooling/on) are shown in Figure 3. The upper limit $u_{\max}^{\text{slow}}$ is defined as the slow component of $Q^{-1}\cdot\vec{x}^{+}$ and $u_{\min}^{\text{slow}}$ is the slow component of $Q^{-1}\cdot\vec{x}^{-}$. This choice ensures that a hysteresis controller implemented in $\vec{u}$-coordinates has the same steady state solution as the regular hysteresis controller. Lines corresponding to the limit values $u_{\max}^{\text{slow}}$ and $u_{\min}^{\text{slow}}$ (transformed to $\vec{T}$-space) are illustrated in Figure 3.

B. Limits on the fast mode

Having determined control limits for $u^{\text{slow}}(t)$, we determine the resulting bounds on $u^{\text{fast}}(t)$ for *arbitrary* admissible control signals $s(t)$, referring to the symbols in Figure 3.

We first identify the minimum values of $u^{\text{fast}}(t)$. In our example, this occurs when the case temperature is lower than the food temperature. The largest difference can be achieved by letting the case and food first warm to the highest temperature permitted by (9). This occurs at the point $\vec{y}^{+}$, where $T_c = T_f$ and $u^{\text{slow}}(t) = u_{\max}^{\text{slow}}$ (using (6a)). Switching on the compressor at this point results in a rapid cooling of the case with respect to the food. The corresponding trajectory $\phi(t;\vec{y}^{+},1)$ represents the minimum-u^{fast} solution. It intersects the line $u^{\text{slow}}(t) = u_{\min}^{\text{slow}}$ at point $\vec{z}^{-}$.

Second, a analogous process is used to identify the maximum values of $u^{\text{fast}}(t)$. The highest values occur when the case is warmer than the food; this difference can be maximised by cooling the food to the fullest extent before switching off the compressor and allowing the case to heat up. This results in the points $\vec{y}^{-}$ and $\vec{z}^{+}$ and the connecting trajectory.

Together, the lines $u^{\text{slow}} = u_{\max}^{\text{slow}}$, $u^{\text{slow}} = u_{\min}^{\text{slow}}$ and the trajectories between $\vec{y}^{-}$ and $\vec{z}^{+}$ and between $\vec{y}^{+}$ and $\vec{z}^{-}$ span an accessible temperature envelope Ω_T. If temperatures within the envelope are not acceptable to the system designer, this may warrant adjusting the constraints (9).

IV. Decentralized controller

Nondisruptive decentralised control of the first order system (9)-(10) can be implemented using the stochastic controller that was recently proposed by Tindemans *et al.* [3] and further extended in [8]. In summary, its key properties are as follows.

- The aggregate power consumption P_{total} of a large *heterogeneous* population is modulated by a control signal $\Pi(t)$. $\Pi(t)$ specifies the power consumption relative to the steady state ($\Pi(t)=1$ is normal operation). It can be chosen freely, subject to power and energy constraints.
- Each appliance receives the signal $\Pi(t)$, which signifies the *global control intent*. The signal does not need to be sent to the appliances in real time: it may be transmitted ahead of time as a schedule, or the device can contain an internal model to compute $\Pi(t)$, for example as a function of grid frequency.
- Each appliance independently constructs a probabilistic model for its control actions. Notably, in this step the device ignores its current temperature and on/off state, but enforces temperature constraints (9) and the targeted average power consumption $\Pi(t)$. The controller modulates the accessible range of $u^{\text{slow}}(t)$ by introducing a variable lower temperature bound $u_{\text{low}}^{\text{slow}}(t)$ that is more restrictive than the hard limits imposed by (9).
- Stochastic control actions (i.e. switching on/off) are determined on the basis of the current device temperature $u^{\text{slow}}(t)$. The result of the control scheme is that the *expected* power consumption of appliance a equals the target value: $E[P^a(t)] = \Pi(t)P_{\text{avg}}^a$. Independence between appliances and the law of large numbers guarantee that the aggregate power consumption tracks $\Pi(t)$.

V. Results

The control strategy specified above has been applied to a homogeneous population of 10,000 simulated appliances using the parameters (3) and (8) (approximately enforced using (9)).

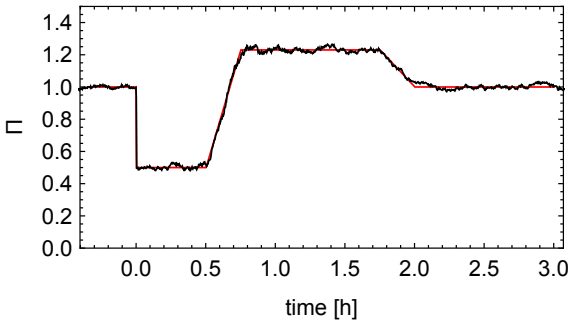

Fig. 4. Simulated relative power consumption of a collection of $N = 10\,000$ second order refrigerator models. The aggregate power consumption (black trace) closely tracks the control signal (red line).

Figure 4 shows an example where the aggregated refrigerators provide frequency response services (secondary frequency response in the GB context). Their aggregate power consumption is reduced to 50% of the steady state level, and this is maintained for 30 minutes, after which a controlled payback period is initiated. The red line shows the reference signal, and the black line depicts the simulated aggregate power consumption (relative to the steady state level) of 10,000 refrigerators.

Figures 5 and 6 illustrate the nondisruptive nature of the proposed controller. Figure 5 shows the temperature trace of a single refrigerator in the population. It stays within the temperature envelope Ω_T at all times, despite large swings in aggregate power consumption. Similarly, Figure 6 shows snapshots of 200 appliance temperatures at five stages during the control cycle shown in Figure 4. In addition to the nondisruptive nature of the controller, this figure illustrates how the accessible temperature domain is temporarily restricted during

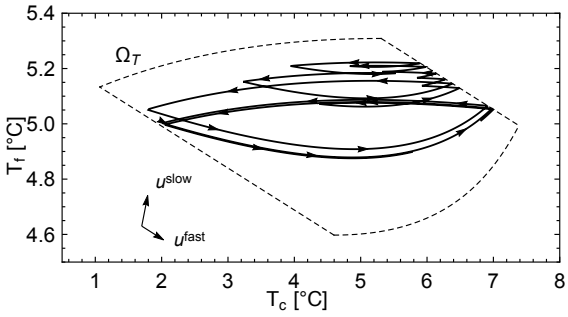

Fig. 5. Temperature dynamics of a second order refrigerator model subjected to the power modulation control signal shown in Figure 4. The dotted line delineates the accessible temperature envelope Ω_T.

the provision of frequency services (dashed line). The full temperature envelope is accessible again after the payback period (final snapshot). Finally, Figure 2 ($t > 0$) illustrates the qualitative difference between nondisruptive control for first and second order models, for a similar power profile $\Pi(t)$.

VI. Conclusions and Further Work

We have demonstrated that a definition of nondisruptiveness in terms of a system's slow temperature mode results in simplified control using an embedded first order system. This enables the use of an advanced stochastic controller [3] for decentralised and accurate control of the aggregate power consumption. To implement this controller, appliances will need to estimate both their thermal models and slow mode temperature $u^{\text{slow}}(t)$. Future work will consider the impact of inevitable errors in the estimation process on both the aggregate power consumption and quality of service.

Acknowledgment

The authors thank Vincenzo Trovato and Paola Falugi.

References

[1] D. S. Callaway and I. A. Hiskens, "Achieving Controllability of Electric Loads," *Proceedings of the IEEE*, vol. 99, no. 1, pp. 184–199, jan 2011.

[2] M. Kamgarpour, C. Ellen, S. E. Zadeh Soudjani, S. Gerwinn, J. L. Mathieu, M. Nils, A. Abate, D. S. Callaway, M. Fränzle, and J. Lygeros, "Modeling Options for Demand Side Participation of Thermostatically Controlled Loads," in *2013 IREP Symposium*. Rethymnon (GR), 2013.

[3] S. H. Tindemans, V. Trovato, and G. Strbac, "Decentralized Control of Thermostatic Loads for Flexible Demand Response," *IEEE Transactions on Control Systems Technology*, vol. 23, no. 5, pp. 1685–1700, sep 2015.

[4] W. Zhang, J. Lian, C.-Y. Chang, and K. Kalsi, "Aggregated Modeling and Control of Air Conditioning Loads for Demand Response," *IEEE Transactions on Power Systems*, vol. 28, no. 4, pp. 4655–4664, nov 2013.

[5] V. Trovato, S. H. Tindemans, and G. Strbac, "Controlling the synchronization and payback associated with the provision of frequency services by dynamic demand," in *CIRED 2013*. Stockholm (SE), 2013.

[6] B. Ramanathan and V. Vittal, "A Framework for Evaluation of Advanced Direct Load Control With Minimum Disruption," *IEEE Transactions on Power Systems*, vol. 23, no. 4, pp. 1681–1688, nov 2008.

[7] J. L. Mathieu, S. Koch, and D. S. Callaway, "State Estimation and Control of Electric Loads to Manage Real-Time Energy Imbalance," *IEEE Transactions on Power Systems*, vol. 28, no. 1, pp. 430–440, feb 2013.

[8] V. Trovato, S. H. Tindemans, and G. Strbac, "Leaky storage model for optimal multi-service allocation of thermostatic loads," *IET Generation, Transmission & Distribution*. [in press]. doi: 10.1049/iet-gtd.2015.0168

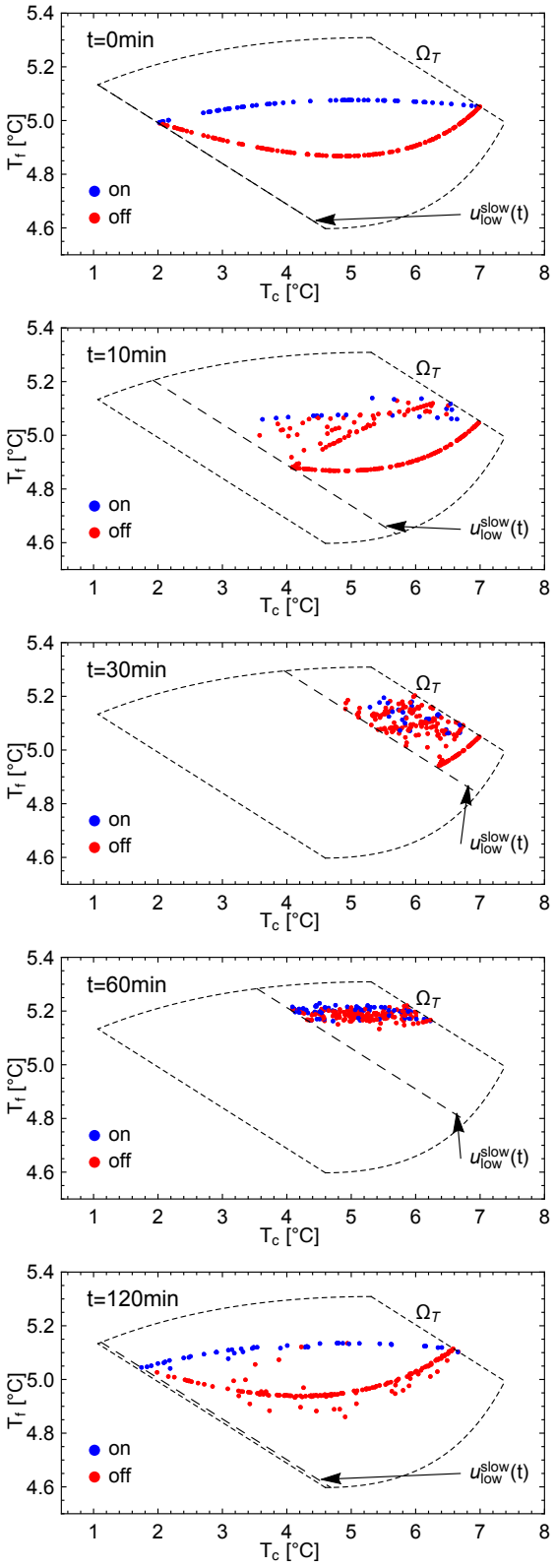

Fig. 6. Snapshots of temperatures of 200 refrigerators with random initial conditions. Appliances in the *on* state are blue (cooling) and those in the *off* state are red (heating). The accessible temperature envelope Ω_T is shown with a dotted line, and the variable lower bound $u^{\text{slow}}_{\text{low}}(t)$ is shown with a dashed line.